GSICS Global Space-based Inter-Calibration System

Quarterly

Newsletter– Spring 2020 Issue

doi: 10.25923/enp8-6w06
Vol.14 No 1, 2020
Editors: Zoltan Szantoi (EC/JRC)
Valentina Boccia (ESA)
Carine Quang (CS Group)

CMA • CNES • ESA • EUMETSAT • IMD • ISRO • JAA • JMA • KMA • NASA • NIST • NOAA • ROSCOSMOS . ROSHYDROMET • SITP • USGS • WMO

Special Issue on Copernicus Sentinel-2

Articles

Copernicus Sentinel-2 Mission: Calibration and Validation activities
By Valentina Boccia (ESA) and Zoltan Szantoi (European Commission/JRC)

Copernicus Sentinel-2 Mission Overview
By Ferran Gascon (ESA)

Sentinel-2 radiometric calibration : Stability overview for both Sentinel 2 MSI-A and MSI B sensors
By Bruno Lafrance and Ouahid Aznay, (CS Group)

Absolute Calibration of the viewing frames: prediction models utilization for Sentinel 2B
By Alice Chambrelan and Dimitra Touli Lebreton, Airbus Defence and Space

Copernicus Sentinel-2 Level 1 Radiometric assessment Using four Independent Vicarious Cal/Val Methods
By Bahjat Alhammoud (ARGANS Ltd, UK)

Long term monitoring of the absolute geolocation of Sentinel 2 satellites
By Marion Neveu Van Malle and François Guyot (Thales Alenia Space)

Sentinel-2 L2A Surface Reflectance Product compared with Reference Measurements on Ground
By Bringfried Pflug (DLR) and Jérôme Louis (Telespazio France)

Towards harmonization of multi sensor time series: radiometric Top of Atmosphere reflectance consistency assessment
By Sindy Sterckx and Erwin Wolters (Flemish Institute for Technological Research, VITO)

News in This Quarter

The new Copernicus digital elevation model
By Peter Strobl (European Commission/JRC)

Announcements

EUMETSAT Meteorological Satellite Conference 2020 Cancelled
By Tim Hewison (EUMETSAT)

GSICS Related Publications

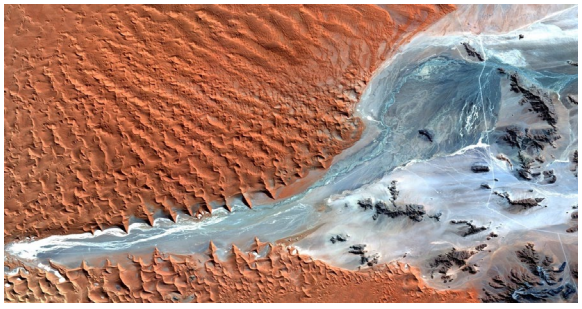

Copernicus Sentinel-2 image over Namibia

Copernicus Sentinel-2 image of Lake Natron

Copernicus Sentinel-2 Mission: Calibration and Validation activities

By Valentina Boccia (ESA) and Zoltan Szantoi (European Commission/JRC)

The Copernicus Sentinel-2 Constellation is composed of two satellites; Sentinel-2A launched in June 2015 and Sentinel-2B launched in March 2017. They both carry on-board a Multi-Spectral Instrument (MSI) sampling 13 spectral bands, from visible to short wave infrared, with four bands at 10m, six bands at 20m and three bands at 60m spatial resolution.

With its free and open data policy, the Copernicus Sentinel-2 Constellation provides users worldwide with Top-Of-Atmosphere (TOA, Level-1C) and Bottom-Of-Atmosphere (BOA, Level-2A) reflectance data, both in cartographic geometry.
Timely provision of Sentinel-2 data allows the scientific community to identify and characterize dynamic surfaces processes, and in particular allows Sentinel-2 products to feed the Copernicus Services (especially for land monitoring, agricultural policy monitoring, emergency management and security, and maritime monitoring) in support of policy makers' decisions. Dr. F. Gascon, the Copernicus Sentinel-2 Mission Manager at ESA, provides a detailed overview of the Constellation in this special issue.

Sentinel-2 data quality is constantly monitored and assessed by the Copernicus Sentinel-2 Mission Performance Center (S2 MPC), with scientific support from the French Space Agency (CNES), and managed by the European Space Agency (ESA) in the ESA-ESRIN site in Frascati (Italy). The calibration and validation activities are routinely carried out in order to make sure that Sentinel-2 data fulfill the mission requirements set by the European Commission. This includes both geometric and radiometric Cal/Val activities, for both Level-1C and Level-2A data, as well as cross-mission validation activities with other, well-known satellite data (e.g., Proba-V). More details on the specific methodologies implemented to ensure a timely and routinely calibration and validation of Sentinel-2 data can be found in this GSICS special issue, with several articles written by S2 MPC members. Additionally, dedicated Data

doi: 10.25923/enp8-6w06

Quality Reports are published every month on the ESA Sentinel Online website (https://sentinels.copernicus.eu/web/sentinel/data-product-quality-reports) and a historical archive is also maintained. The quality and reliability of Sentinel-2 data, provided by the MSI sensor, are currently considered as a reference data/sensor by the broad international scientific community. In fact, several studies have been carried out worldwide, where inter-comparison of other satellite data with Sentinel-2 data has been explored. In order to ensure that Sentinel-2's data quality is always up to its required level, the Sentinel-2 Quality Working Group (S2QWG) has been constituted. The S2QWG monitors the most reliable and internationally recognized techniques, and based on those recommends data quality improvements, which are periodically implemented on the various Sentinel-2 products. The S2QWG members include several actors, such as ESA, the S2 MPC, the European Commission, the Copernicus Services, and other International Space Agencies.

Additionally, the Sentinel-2 Validation Team (S2VT) meeting is also organized by ESA once a year. This event is open to anyone interested in the topic, and it is aimed at gathering together the international validation community to discuss Sentinel-2 data quality-related matters and validation activities, often carried out by teams external to the dedicated S2 MPC. The recommendations provided by the S2VT participants are collected and then reviewed by ESA and the S2QWG for potential implementation.

This special GSICS Newsletter issue comprises seven articles: the first, written by *Gascon* introduces the Copernicus Sentinel-2 mission and the others focus on the calibration and validation activities performed by the S2 MPC. In the calibration domain, *Lafrance* & *Aznay* present the stability of the radiometric calibration results for Sentinel-2 MSI-A and MSI-B sensors, and *Chambrelan* & *Touli-Lebreton* describe the Absolute Calibration of the Viewing Frames as one of the geometric calibration activities for the S-2 constellation. *Alhammoud* introduces four vicarious calibration/validation methodologies for earth observation optical sensors: Rayleigh scattering, Desert PICS, Ground-based TOA-reflectance and Sensor-to-sensor inter-calibration, and their application on the S-2 Constellation with the DIMITRI-toolbox. *Sterckx* & *Wolters* show results from a desert calibration activity for Landsat 8, PROBA-V, Deimos-1, S2A, and S2B. Regarding the Validation activities, *Neveu Van Malle* & *Guyot* focus on the long-term monitoring of the absolute geolocation of both satellites and the short and long-term variations observed. Finally, *Pflug* & *Louis* show an essential ground reference for validation of atmospheric correction algorithms to produce Sentinel-2 L2A Surface Reflectance Products.

Discuss the Article

Copernicus Sentinel-2 Mission Overview

By Ferran Gascon, ESA

Copernicus [www.copernicus.eu] is the European Union's Earth Observation Programme, looking at our planet and its environment for the ultimate benefit of all European citizens. It offers information services based on satellite Earth Observation and in situ (non-space) data.

The Programme is coordinated and managed by the European Commission. It is implemented in partnership with the Member States, the European Space Agency (ESA), the European Organisation for the Exploitation of Meteorological Satellites (EUMETSAT), the European Centre for Medium-Range Weather Forecasts (ECMWF), EU Agencies and Mercator Océan.

The space segment of the Copernicus Programme includes the Sentinels family of satellites. The European Space Agency (ESA) is responsible for coordinating the operations of the Sentinels missions from the data sensing acquisition to the products dissemination to the users and is in charge of ensuring the respective products quality's standards.

The Sentinel-2 mission consists on a Multi-Spectral Instruments (MSI) on board a constellation of two satellites: Sentinel-2A launched in June 2015 and Sentinel-2B launched in March 2017. The mission, with its two satellites, covers the Earth's land surfaces and coastal waters every five days under the same viewing conditions and every three days at mid-latitudes with high spatial resolution and a wide field of view 5-day revisit (i.e. under same viewing conditions) is met at all latitudes of observations (not only at equator), and with the swath overlap and the S2 orbit repeat pattern (14+3/10 rev/day, i.e. a 3 day sub-cycle), 3 day geometric coverage is achieved at mid latitudes.

Return to Page One

doi: 10.25923/enp8-6w06

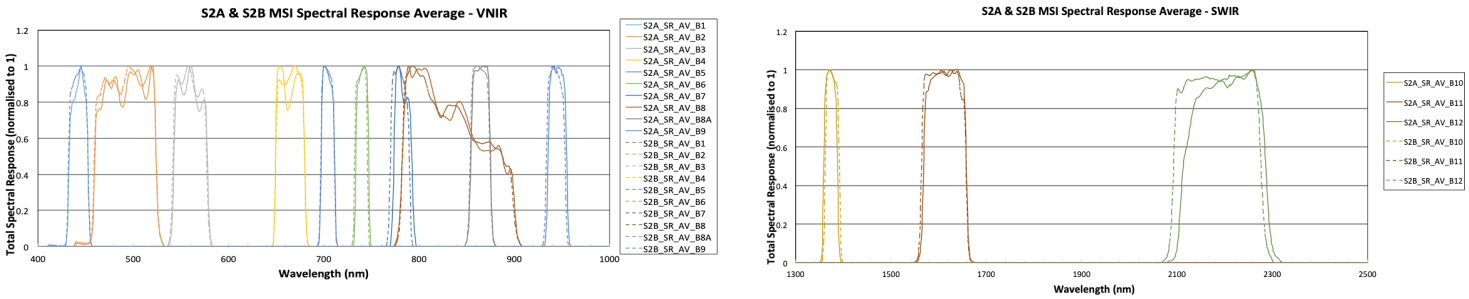

Figure 1: Sentinel-2A and Sentinel-2B spectral bands. Sentinel-2A responses are represented by a solid lines and Sentinel-2B by a dashed lines.

The MSI samples 13 spectral bands (from visible to short wave infrared spectrum): four bands at 10 m, six bands at 20 m and three bands at 60 m spatial resolution (cf. Figure 1). The Sentinel-2 mission provides systematic coverage of all regions depicted in Figure 2.

All Sentinel-2 data products are available to users under a free and open data policy, which underpins the development of long-term, sustainable EO applications.

Sentinel-2 core products available for users are Level-1C (top-of-atmosphere reflectances in cartographic geometry) and Level-2A (surface reflectances in cartographic geometry). For both Level-1C and Level-2A, the product granularity consists of squared tiles, each one composed by 100x100 km^2 ortho-images in UTM/WGS84 projection.

The operational provision of globally and temporally consistent data provided by Sentinel-2 allows a detailed characterization of dynamic surface processes from national to continental scales.

In particular, Sentinel-2 provides relevant data feeding services for applications in the Copernicus priority areas of:

- **Land monitoring**: the regular availability of Sentinel-2 data over all of the land masses allows the continuous update of the Land Cover mapping with unprecedented rapidness and accuracy. Illegal logging and deforestation are examples of the activities that can be closely monitored.

- **Common Agricultural Policy monitoring**: thanks to the increased revisit time of Sentinel-2 and the presence of dedicated spectral bands, Sentinel-2 data is being extensively adopted by the European national entities for monitoring agricultural practices like crop classification, vegetation growth and harvesting.

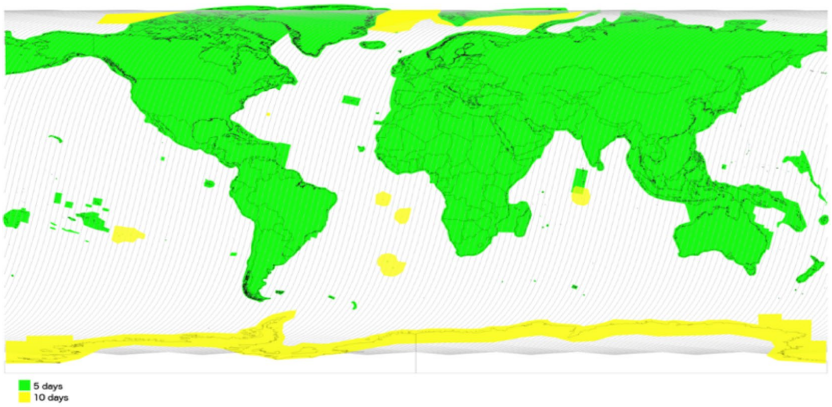

Figure 2: Sentinel-2 nominal observation scenario, in green regions covered with 5-day revisit periodicity, in yellow regions covered with 10-day revisit periodicity.

Figure 3: Sentinel-2 image over green algae blooms swirling within the Baltic Sea.

Return to Page One

doi: 10.25923/enp8-6w06

- **Emergency management and Security**: the potential offered by the Sentinel-2 series, in terms of dense time series of data, nurtured the development of new and advanced techniques for the joint analyses and exploitation of high-frequency time series of data devoted to the disaster's management and mitigation such as forest fires, floods and situational awareness.
- **Maritime monitoring**: by providing accurate coastal water products such as turbidity and bathymetry (Figure 3); in addition, the coverage of Arctic and Antarctic seas allows accurate monitoring of glaciers and iceberg.

An ever-growing variety of new applications is constantly stimulated by the Sentinel-2 data availability covering scientific and operational thematic areas such as geology, mining, fishery, biodiversity, energy oil and gas management, water resource management, urban monitoring, etc.

Discuss the Article

Sentinel-2 radiometric calibration : Stability overview for both Sentinel-2 MSI-A and MSI-B sensors

By Bruno Lafrance and Ouahid Aznay (CS GROUP, France)

The Sentinel-2 MSI sensors are calibrated monthly by the Copernicus Sentinel-2 Mission Performance Centre (MPC), from specific calibration images: acquisitions over ocean at night for the dark signal calibration, on-board sun diffuser images for the absolute radiometric calibration and the pixel equalization. The principles of radiometric calibrations are fully described in *Gascon et al., 2017* and summarized in *Lamquin et al., 2019.* In order to maintain a high level of quality of the Sentinel-2 products, the monthly calibration leads to an update of the dark signal coefficients and also absolute and relative gain coefficients used by the Level-1 processing chain. The mission requirements aim to achieve a radiometric uncertainty lower than 5% as limit threshold and 3% as goal of ideal accuracy. It is part of the radiometric validation activity to assess the final accuracy of the sensor calibration.

The dark signal has remained quite stable for both MSI-A and MSI-B sensors, since they have been in-flight. The dark signal variations are smaller than 0.5 digital counts for most of the VNIR pixels and lower than 1 digital count for most of the SWIR pixels, i.e. in the range of the dark noise. The dark signal calibration is relevant to detect new defective pixels. Up to now, MSI-A has lost only eight pixels in SWIR bands when MSI-B has lost only two pixels, which became defective. As SWIR bands possess multi-line detectors made of three or four lines (three lines for the B10 band, four lines for the B11 and B12 bands), a pixel-dependent reselection of the defective pixels is possible. Such a reselection was performed for MSI-A with success for five pixels which are still currently operational.

The absolute and relative gain coefficients are estimated from sun-diffuser acquisitions by comparing the measurements to the simulations of the reflected radiance. The monitoring of the sensitivity of the radiometric response is an important output of the calibration activity as the update of the absolute calibration coefficients ensures to maintain a constant level of the measured radiance over the duration of the mission. The time evolution of the absolute calibration coefficients is illustrated in Figure 1 for the VNIR bands of MSI-A and MSI-B. For each spectral band, the plots show the relative variation of the absolute gains with respect to their first estimate on-flight, in percent.

Since the first in-orbit calibration, calculations have been showing a trend of sensitivity loss over time for MSI-A VNIR bands (between -0.6% and -1.4% depending on the spectral band).

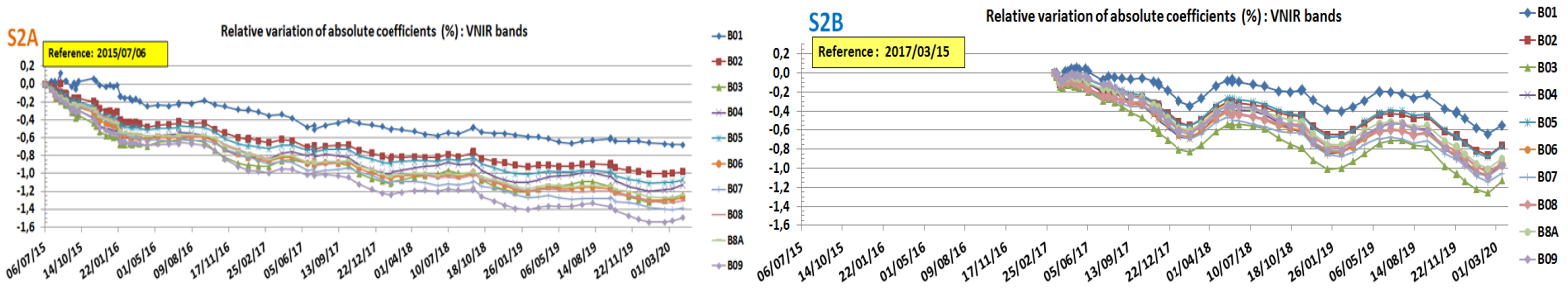

Figure 1: Time variation of the absolute calibration coefficients, for VNIR bands, normalized by the first coefficient (i.e. from the sun-diffuser acquisition on July 6th 2015 for MSI-A, on March 15th 2017 for MSI-B).

doi: 10.25923/enp8-6w06

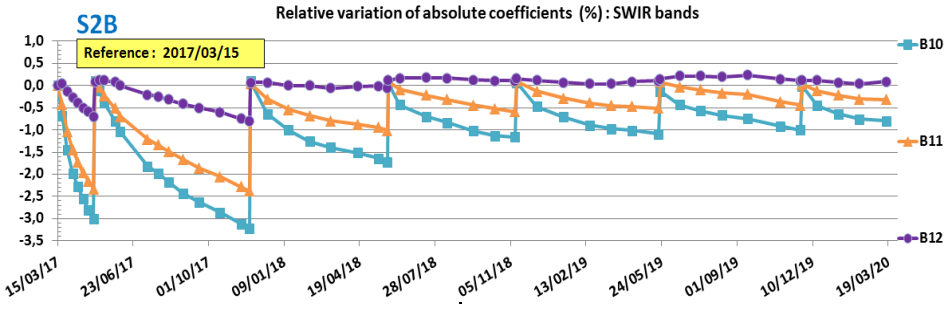

Figure 2: Time variation of the absolute calibration coefficients, for SWIR bands of MSI-B, normalized by the first coefficient.

The decrease is mainly apparent during the first two years in orbit. Since July 2017, it has been less important (only -0.2% to -0.4% depending on the spectral band). A small seasonal effect is also observed, which is correlated with the limited accuracy of the sun-diffuser BRDF model. For MSI-B VNIR bands, the rate of loss of sensitivity is similar to that of MSI-A, but with a stronger seasonal effect with oscillations twice as large as those for MSI-A (~0.30% peak-to-peak for MSI-B versus ~0.15% for MSI-A). These oscillations are small with respect to the mission requirements (3% uncertainty target). They are due to residual uncertainties on the characterization of the sun-diffuser BRDF. We also notice the time variation for the absolute gain of the B01 band is different than for the other bands. And, for MSI-B there is a clear oscillation with time for the absolute calibration of B01 which is not as apparent for MSI-A.

Let's note, MSI sensors are equipped with only one onboard solar diffuser per satellite. There is no possibility to monitor the solar diffuser ageing with respect to a second diffuser which should be used less often, as for Landsat-8 for instance. Up to now, there is no suspicion of solar diffuser degradation, because such an effect should mainly impact the B1 band. But, its lower decrease of sensitivity than for the other bands does not reflect an effect of sun-diffuser ageing. Moreover, according to Airbus Defence and Space, in charge of the sensor manufacturing, the cumulative exposure of a sun-diffuser will be 51 min over the nominal lifetime and 1h28min over extended lifetime, while the qualification limit of the sun-diffuser stability to an UV exposure (responsible for its ageing) has been estimated to be 2h00 (V. Samson and V. Chorvalli, 2015).

For SWIR bands, there is a faster decrease of the absolute calibration coefficients with time (see Figure 2 for MSI-B). The largest decrease happens for the B10 band, followed by the decrease of the B11 band, as foreseen for these bands which are sensitive to water vapour contamination. Regular decontamination activities allow restoring the value of the absolute calibration coefficients for SWIR bands and gradually reduce the rate of decrease. They are now performed once a year for MSI-A, in order to respect a conventional threshold of 3% for a maximum decrease of sensitivity. The frequency of decontaminations is twice a year for MSI-B (for which the periodicity of one year will be soon achieved).

The degradation of the sensor equalization is assessed for each calibration sequence by calculating the Fixed Patter Noise (FPN). This estimate is based on the conversion of the sun-diffuser acquisition to level 1B (equalized image) by applying the current operational relative gain coefficients (from the previous calibration sequence). The FPN thresholds are estimated for the radiance level of sun-diffuser observations (at Lmax / 2), assuming a linear variation of the FPN between Lref and Lmax, for which the requirements are defined. Except in case of a very punctual change of the relative gain coefficients (for instance in case of a dust deposit), the FPN is very below the threshold (0.2%) for all VNIR bands. The threshold is also 0.2% for the B11 and B12 bands but 0.35% for the B10 band. For SWIR bands, even if the change of inter-pixel response is more pronounced than for VNIR bands, most of FPN values are below the threshold. Sometimes the FPN exceeds the threshold when there are strong local changes of response for few pixels. The monthly update of relative gain coefficients, both for WIR and VNIR bands, at the same time, ensures that the FPN will again meet requirements.

References:

F. Gascon, et al, « **Copernicus Sentinel-2A Calibration and Products Validation Status** », Remote Sensing, 2017, Volume 9(6) (https://doi:10.3390/rs9060584).N.

Lamquin, **et al**, « An inter-comparison exercise of Sentinel-2 radiometric validations assessed by independent expert groups », Remote Sensing of Environment, 2019, Volume 233 (https://doi.org/10.1016/j.rse.2019.111369).

V. Samson and V. Chorvalli, « **Sentinel-4A LEOP & In-Orbit Verification Report, Annex 8 – MSI Performances** », Airbus Defence & Space report, GS2.RP.ASF.MSI.00224, version 1, September 25th 2015.

Return to Page One

Discuss the Article

doi: 10.25923/enp8-6w06
GSICS Quarterly: Spring Issue 2020 Volume 14, No. 1, 2020

Absolute Calibration of the viewing frames: prediction models utilization for Sentinel-2B

By Alice Chambrelan and Dimitra Touli Lebreton (Airbus Defence and Space)

The geometric calibration activities are part of the Copernicus Sentinel-2 Mission Performance Centre (MPC) activities managed by ESA. They permit analysis to ensure compliance to the geometric requirements for the Sentinel-2 products: mainly planimetry, length distortion and absolute geolocation performance. Especially important is the absolute calibration of the viewing frames. This consists of the determination of their orientation with respect to a frame linked to the Earth in order to guarantee the absolute geolocation performance. This geometric calibration is based on the refinement of the geometric models by space-triangulation [1]. For Sentinel-2 this calibration is achieved by MPC's L1 Geometric Calibration team (L1_GEO_CAL). Given the high rigidity between Visible to Near-Infrared (VNIR) and Short-Waves Infrared (SWIR) and inside VNIR and SWIR focal planes (validated by inter-band registration analysis), only one band is needed for calibration: the B4 spectral band of L1B products is chosen because it gives the best correlation reference data, typically panchromatic. These products are correlated with Ground Control Points (GCPs) or well-located images to obtain a refined VNIR geometric model.

To perform this calibration, a large number of scenes are used. Indeed, the range of scenes needs to cover a variety of geographic sites all over the world with a good distribution in latitude to ensure the non-dependency of weather conditions and the visibility of a potential dependency on latitude, date or other criteria.

The absolute geometric calibration consists then of the computation of the bias values for roll, pitch and yaw considering all these scenes, in order to update the Ground Image Processing Parameters (GIPP).

Historically these biases are determined during a calibration campaign. The objective of this campaign is to collect the significant amount of data needed to achieve the determination of the bias values. Considering all the points collected, the values for the GIPP update are computed by minimizing the residual errors after bias correction, taking into account the outliers. These calibration campaigns are carried out when requested.

In order to follow bias evolutions more accurately, a regular monitoring of the biases on some products, carefully chosen, has been performed since the beginning of 2019 for Sentinel-2A and since the commissioning phase in 2017 for Sentinel-2B.

The bias values are averaged to obtain roll, pitch and yaw values by scene. These models, regularly updated and improved with new monitoring data, allow a projection for future date, and so, an optimization of the geolocation performance.

Thus the geometric bias values are now determined using these models. These predicted values are then validated by comparisons with some products, which are not used for the model computation.

Sentinel-2B alignment bias evolves faster compared to the changes for Sentinel-2A. Thus Sentinel-2B absolute geometric calibration updates occur more often. The last calibration update was in November 2019 as designated in Figure 1.

The prediction model used for this calibration is a bilinear regression computed with bias data since May 2018 (orange curve on the Figure 1). After analysis, the new values were predicted and optimized for January 1st, 2020.

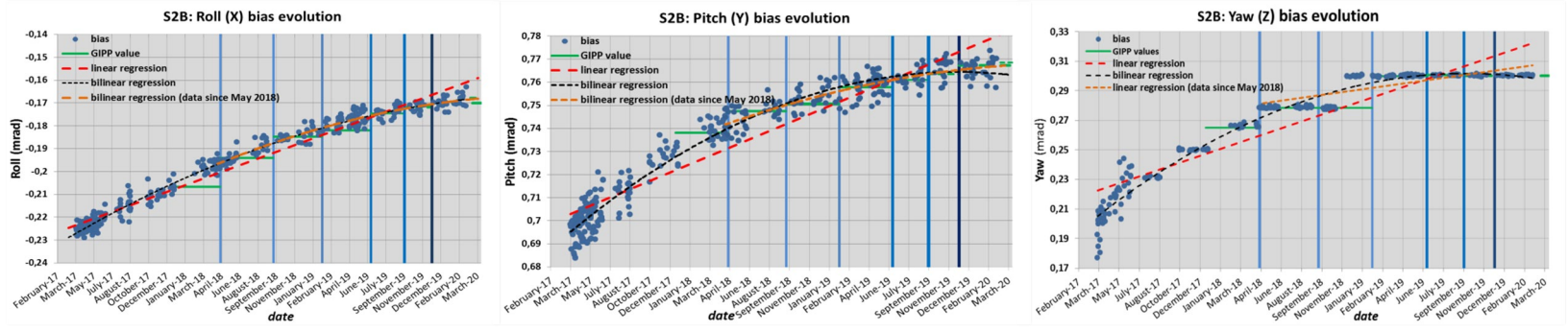

Figure 1: Sentinel-2B bias evolution for (above left to right) roll, pitch and yaw since the launch with prediction models. The vertical lines designate the times of the GIPP updates of the absolute geometric calibrations.

doi: 10.25923/enp8-6w06

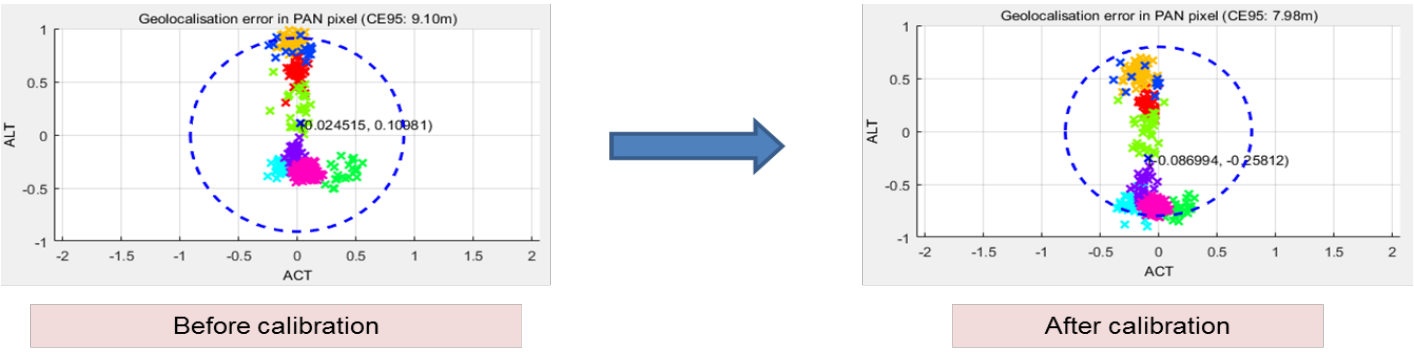

Figure 2: Circular errors computed from eight validation products from November 2019 with the current and the proposed bias values for the calibration of November 2019.

No updated yaw value was proposed for this calibration, the current value was kept. The updated roll and pitch bias values computed with the models were validated by using analysis of measurements over eight regions distributed globally. These validation products were acquired during the beginning of November 2019. For these validation products, along track and across track errors were computed with current and updated bias values as illustrated in Figure 2.

Figure 2 shows the residual errors computed on several points for each validation product. They are represented with the along track error on the vertical axis and the across track error on the horizontal one. The circular error including 95% of all points is also represented. Results give an error of 9.10 meters with the current bias values, and 7.98 meters with the updated roll and pitch values: the geolocation performance is thus improved and this is proved on this set of particular products, validating the new angles bias values.

After the validation done by the MPC team, the updated GIPP was released on 27th November 2019 with the new roll and pitch biases values determined during this described calibration. A check after the updated GIPP release was done by the MPC's L1 Geometric Validation (L1_GEO_VAL) team showing the improvement of the geolocation performance.

Using prediction models for absolute calibration of the viewing frames enables not only improved geolocation performance, but also an anticipation and the optimal future date for the next calibration update, and last but not least, the faculty to be always ready to calibrate.

Reference

[1] Ferran Gascon, Catherine Bouzinac, Olivier Thépaut, Mathieu Jung, Benjamin Francesconi, Jérôme Louis, Vincent Lonjou, Bruno Lafrance, Stéphane Massera, Angélique Gaudel-Vacaresse, Florie Languille, Bahjat Alhammoud, Françoise Viallefont, Bringfried Pflug, Jakub Bieniarz, Sébastien Clerc, Laëtitia Pessiot, Thierry Trémas, Enrico Cadau, Roberto De Bonis, Claudia Isola, Philippe Martimort and Valérie Fernandez, Copernicus Sentinel-2 Calibration and Products Validation Status, Remote Sens. 2017, 9, 584 ; doi:103390/rs9060584

Discuss the Article

Copernicus Sentinel-2 Level-1 Radiometric Assessment Using four Independent Vicarious Cal/Val Methods

By Bahjat Alhammoud (ARGANS Ltd, UK)

The Sentinel-2A and Sentinel-2B constellation is an Earth Observation optical mission developed and operated by the European Space Agency (ESA) in the frame of the Copernicus program of the European Commission. The calibration and validation activities are conducted within the Sentinel-2 Mission Performance Centre (MPC). Four vicarious radiometry validation methods for EO optical sensors have been applied using DIMITRI (Database for Imaging Multispectral Instruments and Tools for Radiometric Intercomparison) toolbox: Rayleigh scattering, Desert Pseudo Invariant Calibration Sites (PICS), Ground-reflectance based and Sensor-to-sensor intercalibration. The results of the validation show an excellent image quality and stable radiometric performance, which meets the mission requirements.

1. Methodology

The radiometry assessment is performed at Level-1C product [1] using the DIMITRI package developed and

Return to Page One

doi: 10.25923/enp8-6w06

maintained by ESA/ESTEC, ARGANS and MAGELLIUM (https://dimitri.argans.co.uk).

1.1 Rayleigh scattering methodology

In ideal conditions—stable oceanic region, with low concentration of phytoplankton and purely maritime aerosol model —Rayleigh scattering can accurately be calculated based on the surface pressure and viewing angles. Hence absolute vicarious calibration can be achieved over the visible spectral range 400-700 nm using open ocean satellite observation [1].

1.2. Desert Pseudo Invariant Calibration Sites (PICS) methodology

PICS method builds a reference reflectance model for the selected site using top-of-atmosphere (TOA) measurements from a reference sensor (MERIS in DIMITRI [2]) and a four-parameters bidirectional reflectance distribution function (BRDF) model for each spectral band. The TOA measurements are computed using the BRDF model and the observation geometry. This method allows performing multi-temporal analysis, as well as comparison of multiple sensors on the same site over the visible to near-infrared (VNIR) spectral range.

1.3. *Ground- Reflectance Based methodology*

This approach has been used to perform the absolute radiometric vicarious calibration for decades [3] and can be summarized by measuring the surface reflectance of the site at the same viewing and solar geometry, and spectral band of the target sensor. Then TOA reflectance of the target sensor is simulated using a radiative transfer model to compute the gain coefficients.

1.4. *Sensor-to-Sensor inter-calibration methodology*

This method assumes the TOA reflectance angular distribution obeys the principle of reciprocity; symmetrical with respect to the principal plane [4]. The strictness of angular matching between observations, cloud percentage, site-coverage percentage and day-offset are user-defined thresholds. The comparison is performed over predefined sites and over similar spectral bands between two sensors.

2. Dataset

2.1. Sentinel-2 Level-1C Products Dataset

The Sentinel-2/MSI Level-1C (L1C) product consists of orthorectified TOA reflectance provided as 110 x 110 km2 tiles, based on the UTM/WGS84 reference frame (https://sentinels.copernicus.eu) with spatial resolution of 10m, 20m and 60m. We use six open ocean sites to perform Rayleigh scattering and six desert sites to perform PICS method in addition to three instrumented reference test sites to perform the Sensor-to-Sensor intercalibration and the ground reflectance-based methods [1]. The entire retrieved dataset until March 2020 is ingested, cloud screened (automatically and manually) and then stored in DIMITRI database to be analyzed.

2.2. *LANDSAT/OLI products*

We use LANDSAT/OLI L1TP products, which are radiometrically and geometrically corrected image and freely available at USGS (https://www.usgs.gov). The ingestion into DIMITRI database has been successfully performed. The dataset is automatically cloud-screened by DIMITRI using Land Automated Cloud Cover Assessment (LACCA) algorithm.

2.3. Ground- Reflectance in-situ measurements

We used the ground-based measurements provided by NASA (Landsat Cal/Val Team) via ESA as part of the ESA-NASA agreement. Seventy-Five cloud-free S2A & S2B overpasses were obtained over the Railroad Valley Playa site (RRVP) over 2015-2019. The TOA normalized reflectance was reconstructed by the University of Arizona team using ground and atmosphere radiometric measurements.

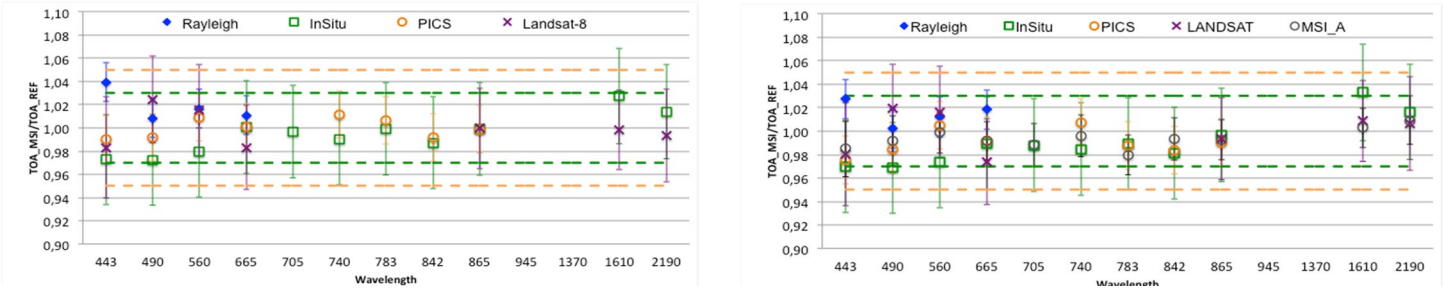

Figure 1: Radiometric gain as the ratio of observed TOA-reflectance to reference TOA-reflectance as a function of wavelength from the four vicarious methods for (Left) Sentinel-2A and (Right) Sentinel-2B (bands B09 & B10 excluded). Error bars indicate the method uncertainty. Orange dashed-line shows the 5% accuracy mission requirement and green dashed-line indicates the 3% accuracy mission target.

doi: 10.25923/enp8-6w06

3. Results and Analysis

Figure 1 presents the synthesis of the results from the four vicarious methods used in this study. The overall gain coefficients (expressed as ratios) are within the 3% target requirements, which provide evidence of the excellent radiometric performance of both S2A and S2B sensors.

Rayleigh Scattering results show that the absolute ratios are within the goal uncertainty of 3% except for B01/MSI-A. The dispersion of the results seems higher for bands B01 to B03 where reflectance is the highest as well as the estimated contributions of Rayleigh and aerosols to TOA signal. The difference between Rayleigh and PICS results over the short wavelength (e.g. B01) is most likely related to the aerosol input. Particularly DIMITRI-model seems to under estimate the Water leaving reflectance, which leads to higher calibration coefficients.

PICS results show that all the ratios are close to unity with higher scattered ratios of short wave lengths (e.g. B01) mainly due to the low surface reflectance and the high contribution of atmospheric signal. However, it has been demonstrated that a stable temporal evolution of both sensors can be seen over the ratios time-series where trend values are less than 1% per year [5].

The results of the Ground-Based Reflectance Measurements show ratios close to unity with bias within 3%. Both sensors display the same spectral shape where the VNIR bands under estimate the TOA signal, while the SWIR bands over estimate it. This spectral shape is still under investigation.

The Cross-Mission Intercomparison between MSI-A vs MSI-B show a slight offset of about 1-2% [5], while the results of the intercomparison with LANDSAT/OLI are consistent up to 2-3%. In spite of the difference of acquisition time and spectral response of MSI to OLI, the three sensors compare well in terms of radiometric measurements and image qualities.

Acknowledgements

This work has been funded by ESA in the framework of Sentinel-2MPC managed by CS-group; and DIMITRI-QA4EO project managed by ARGANS. We gratefully acknowledge the RadCaTS dataset was provided by the NASA Landsat Cal/Val Team as part of the ESA expert users effort.

References

[1] Gascon, F., Bouzinac, C., Thépaut, O., et al., 2017, Copernicus Sentinel-2A Calibration and Products Validation Status, MDPI Remote Sens., 9, 584, 10.3390/rs9060584

[2] Bouvet, M. (2014). Radiometric comparison of multispectral imagers over a pseudo-invariant calibration site using a reference radiometric model, Remote Sensing of Environment 140 (2014)

[3] Slater P. N., Holm R. G., Jackson R. D., et al., (1987), Reflectance- and radiance- based methods for the in-flight absolute calibration of multi-spectral sensors" Remote Sens. Environ. Vol. 22, No. 1, pp: 11-37, June 1987.

[4] Bouvet, M. (2006). Intercomparison of imaging spectrometer over the Salar de Uyuni (Bolivia), Proceedings of the 2006 MERIS AATSR Validation Team Workshop.

[5] Alhammoud, B., Jackson J., Clerc S., et al., 2019. "Sentinel -2 Level -1 Radiometry Assessment Using Vicarious Methods From DIMITRI Toolbox and Field Measurements From RadCalNet Database." IEEE-JSTARS, 12, no. 9. Doi: 10.1109/JSTARS.2019.2936940

Discuss the Article

Long-term monitoring of the absolute geolocation of Sentinel-2 satellites

By Marion Neveu Van Malle and François Guyot (Thales Alenia Space)

The Sentinel-2 satellites, part of the Copernicus programme of the European Commission, provide high spatial resolution (10 to 60 m) optical imagery of all the terrestrial surfaces and coastal waters with a high revisit of five days. Both platforms are equipped with high accuracy pointing facilities, allowing excellent geometric performances of the final products. Thales Alenia Space, as a member of the Mission Performance Centre (MPC) managed by ESA, is in charge of the validation of Level-1 radiometric and geometric performances of Sentinel-2. This paper focuses on the long-term monitoring of absolute geolocation performed since the launch of each satellite.

Methodology

Geolocation performance is assessed at level 1C, meaning for products in cartographic geometry. The assessment is based on detection of Ground Control Points (GCP) in Sentinel-2 images by correlation with a database of accurately localised images spread over the world. The process is performed using Sentinel-2 band B03 as reference band. The GCPs database used is a dedicated high-resolution ortho-images database with geolocation accuracy better than 5m.

Return to Page One

doi: 10.25923/enp8-6w06

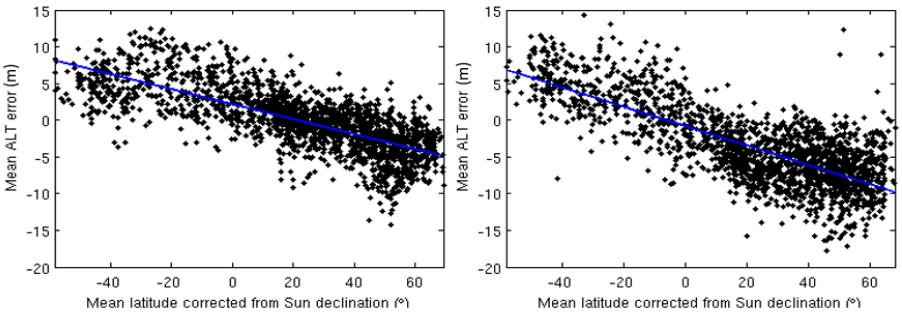

Figure 1. Sun angle dependency of the along-track error for Sentinel-2A (left) and Sentinel-2B (right). Each black dot represents the measurement on a level-1C product. The blue line shows the linear fit of the data, with a computed slope of -0.102 m/° for S2A and -0.132 m/° for S2B.

Short-term and long-term observed variations

The collection of a large amount of data on both satellites has allowed to reveal two main variations of the absolute geolocation: a short-term variation along the orbit and a long-term seasonal variation. It is most likely that both variations are related to thermoelastic effects.

The short-term variations are only visible in the along-track direction. Figure 1 shows the dependency of the measured along-track error as a function of the Sun angle. The Sun angle has been computed by subtracting the Sun declination at the acquisition date of the product to the latitude of the product. The effect is stronger on Sentinel-2B, as shown by the larger slope obtained when computing a linear fit. Note that for Northern products (corresponding to a positive Sun angle) the along-track error is larger for Sentinel-2B. This introduces a bias between Sentinel-2A and Sentinel-2B products acquired during the same period.

The long-term variations of the along-track, across-track and circular errors are shown in Figure 2. While the seasonal oscillations are clearly visible for Sentinel-2A (left panel), they are not that obvious for Sentinel-2B (right panel) due to the regular calibrations applied.

For Sentinel-2A, the along-track error oscillates between +12m and -12m, staying within the targeted performance of 12.5m. For Sentinel-2B, the thermoelastic effects appear to be stronger. The seasonal effects added to the orbital effects are too large to remain within the targeted performance. Regular calibrations of the spacecraft line-of-sight biases need to be applied. In the across-track direction, the evolution seems dominated by a slow drift. On Sentinel-2A, a calibration adjustment of the roll was needed in January 2019 in order to remain within the targeted performance. After a year since this calibration, a seasonal variation seems visible. For Sentinel-2B, the drift of the across-track error seems to have stabilised as well since the calibration of June 2019.

The close monitoring of the absolute geolocation of both satellites, triggering calibrations when needed, ensures that the performance remains within the target of 12.5m (as shown on the lower panels). Note that this target was initially defined assuming that an additional processing of refining over a reference would be activated.

Impact on co-registration and expected improvement with refinement

The calibration strategy currently applied by the Sentinel-2 MPC ensures a good absolute geolocation performance. The short and long-term variations presented here are responsible for the limited co-registration performances affecting users. The short-term variations induce mis-registrations between Sentinel-2A and Sentinel-2B products over short timescales. The long-term variations induce mis-registrations between products from the same satellite over long timescales.

The refinement process, currently under validation, will co-register all the Sentinel-2 products with a common reference, the Global Reference Image (GRI). The GRI has been built from Sentinel-2 data with geometric parameters corrected using GCPs. The thermoelastic effects affecting Sentinel-2 geolocation have been removed from the GRI products. The activation of the refinement in the operational processing of Sentinel-2 level 1C products will compensate for the variations currently observed.

Sentinel-2 geometric performance is currently ensured by periodically adjusting viewing angle biases when the measurements exceed the target. Geolocation performance represents the absolute location performance as provided by the system, and depends uniquely on the calibrated imaging parameters.

Return to Page One

doi: 10.25923/enp8-6w06

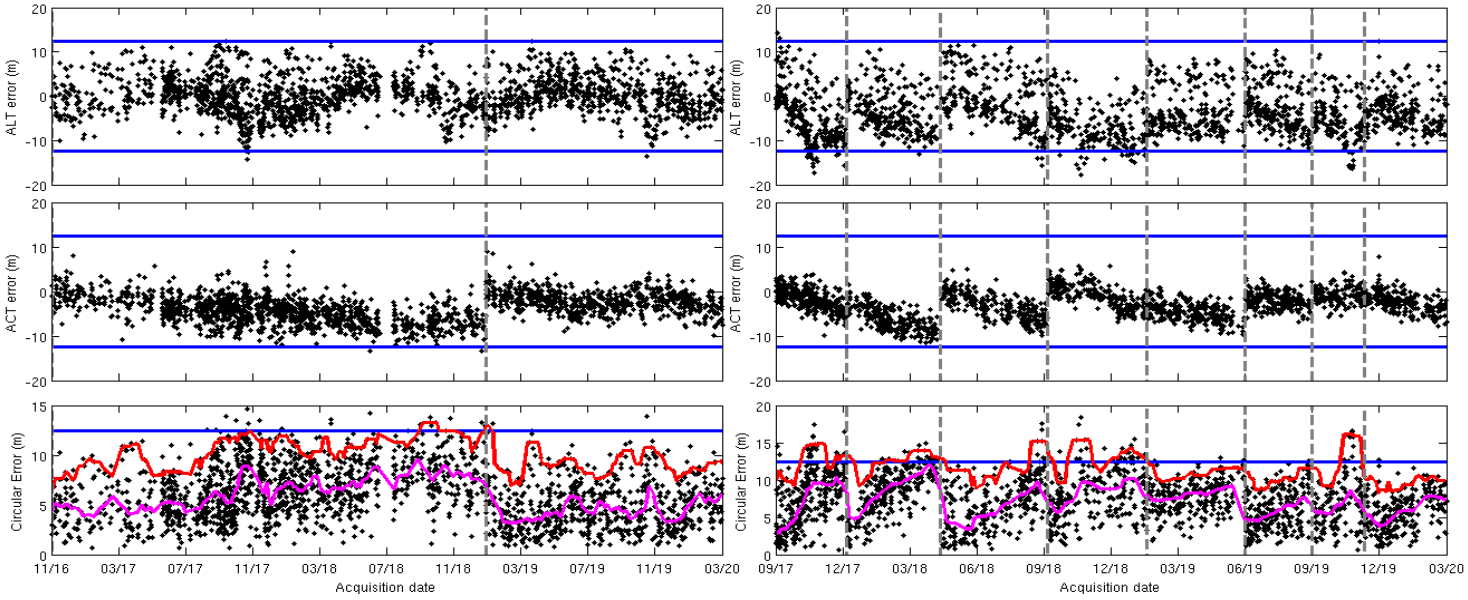

Figure 2. Long-term evolution of Sentinel-2 absolute geolocation. Left: Sentinel-2A. Right: Sentinel-2B. Top: Along-track error in meters. Middle: Across-track error in meters. Bottom: Circular error in meters. Each black dot represents the measurement on a level-1C product. The blue lines show the targeted performance of 12.5m. The vertical dashed lines show the spacecraft line-of-sight calibrations. The purple (resp. red) line shows the median (resp. 95 percentile) of the circular error computed over a sliding window of 30 days.

The co-registration of Sentinel-2 products will be significantly improved, allowing users to work more efficiently on time-series.

References

Drusch, M., del Bello, U., Carlier, S., Colin, O., Fernandez, V., Gascon, F., Hoersch, B., Isola, C., Laberinti, P., Martimort, P., et al., 2012, Sentinel-2: ESA's Optical High-Resolution Mission for GMES Operational Services, Remote Sens. Environ., 120, 25–36, 10.1016/j.rse.2011.11.026

Gascon, F., et al. 2017, Copernicus Sentinel-2A Calibration and Products Validation Status, MDPI Remote Sens., 9, 584, 10.3390/rs9060584

Francesconi, B., et al., 2017, Image quality validation of Sentinel 2 Level-1 products: performance status at the beginning of the constellation routine phase, Proc. SPIE 10423, Sensors, Systems, and Next-Generation Satellites XXI, 1042306, 10.1117/12.2276847

Discuss the Article

Sentinel-2 L2A Surface Reflectance Product compared with Reference Measurements on Ground

By Bringfried Pflug (DLR) and Jérôme Louis (Telespazio France)

1. Introduction

Copernicus Sentinel-2 data are applied for a wide field of applications on land surface related to agriculture, forestry and land-cover change [1-4]. They are also used to monitor coastal and inland waters [5, 6]. Most of these applications require an accurate atmospheric correction, which is provided by Level-2A processor Sen2Cor [7]. Sen2Cor is and identifying clear land surface

2. Sentinel-2 L2A Products

pixels, water areas and pixels covered used by ESA for systematic global Level-2A processing of Sentinel-2 acquisitions. In addition, it can be downloaded from ESA website (http://step.esa.int/main/third-party-plugins-2/sen2cor/sen2cor_v2-8/) as standalone tool for individual processing by the users.

Sen2Cor is applied to correct mono-temporal Copernicus Sentinel-2 Level 1C products from the effects of the atmosphere in order to deliver radiometrically corrected surface reflectance (SR) images. Sen2Cor processing chain starts with the scene classification (SCL) algorithm, which provides a mask of 11 classes for masking out pixels covered by clouds by snow. Average omission errors for

Return to Page One

doi: 10.25923/enp8-6w06

classes clear land, water and snow are 3%, 2% and 4% respectively and average commission errors are 6%, 3% and 1% respectively. However, omission errors can exceed 10% and commission errors can exceed 20% for individual images. Some scene classification evolutions in preparation for the next release of Sen2Cor have the objective to reduce these errors.

The atmospheric correction process starts with estimation of atmospheric aerosol content based on a dense dark vegetation (DDV)-algorithm[7] except when DDV-pixels are not present in the image. The fall-back solution for that case is to use a default value or, if available, to get aerosol content from CAMS data [8]. Next step is the retrieval of water vapour column estimate using the APDA algorithm [9]with Sentinel-2 band B08A and band B09. With this information on atmospheric aerosol content and water vapour content, the top-of-atmosphere (TOA) reflectance is converted to surface reflectance (bottom-of-atmosphere; BOA) [7]. The data format of the Level-2A product [10] follows the structure of the Level-1C product. Level-2A products provide a scene classification map derived from Sentinel-2 data together with cloud and snow probabilities, aerosol optical thickness at 550 nm (AOT550), water vapour (WV) map and surface (BOA) reflectance images.

3. Reference Measurements

Surface reflectance measurements on ground in parallel to Copernicus Sentinel-2 overpasses provide an essential reference for validation of atmospheric correction algorithms. Those measurements were performed in May 2018 and August 2019 by German Aerospace Center in Northern Germany near Lake Stechlin (lon: 13.030E, lat: 53.155N). Meteorological conditions had been perfect in 2018 with cloudiness of 0% in the 9 x 9 km^2 vicinity of the measurement location. Cloudiness was only 1% in that region of interest (ROI) in 2019; however, few small clouds crossed the ROI some minutes before the overpass. The test area represents flat terrain containing mainly meadows and forests. SVC spectrometer HR-1024i [11] was placed over different points on meadows measuring surface reflection relative to the reflection of a white disk. Raw data were corrected for the real reflection of the white disk before comparing with Sentinel-2 SR retrievals. SR measurements on ground with spectrometers like SVC give information about a footprint smaller than a Sentinel-2 pixel. Therefore, average of more than 30 spectra recorded at locations distributed over the area corresponding to one Sentinel-2 pixel was computed for upscaling. Whereas in 2018 measurements are available on a single pixel over a meadow, in 2019 measurements were performed on a dry meadow location and on a nearby wettish meadow location.

AOT spectra, vertical ozone column content and water vapour were measured with Microtops sunphotometers [12] additional to SR measurements. Sunphotometer measurements were averaged over ±15 min to satellite overpass time to give reference values.

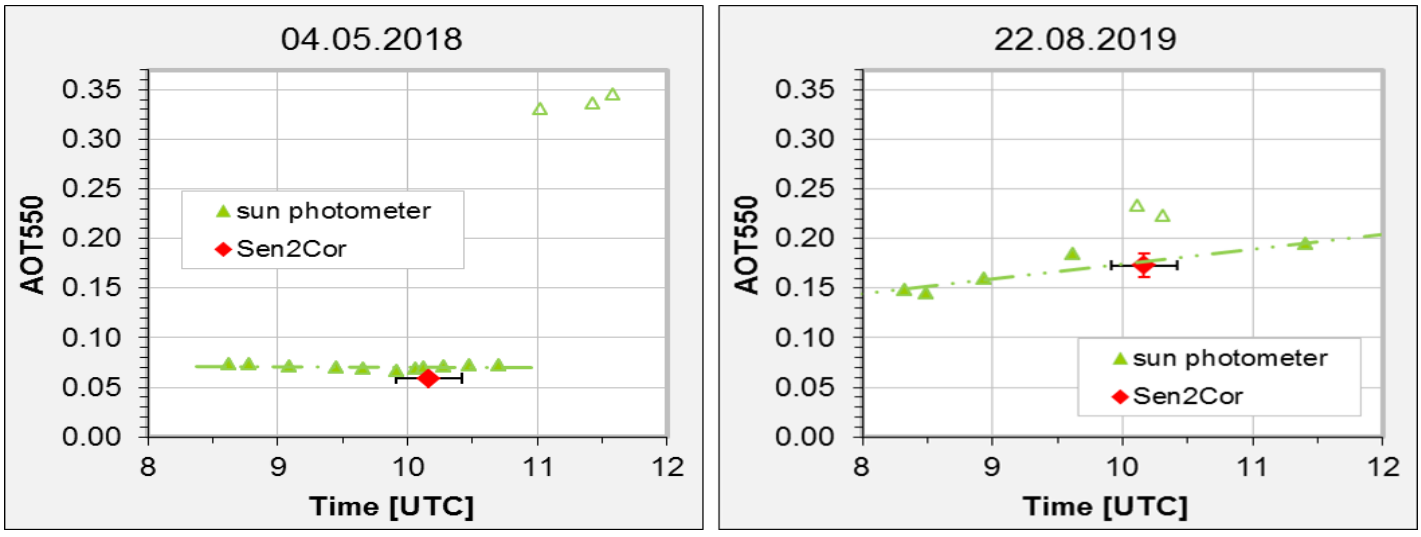

Figure 1: Time variation of vertical column AOT_{550} for overpass days. Filled triangles mark the sun photometer measurements used for interpolation of the trend lines (green dash dot line). Empty triangles are sun photometer measurements excluded from trend line interpolation. The black "error bar" marks the time interval ±15 min to overpass time used for time-averaging of sun photometer data.

Return to Page One

doi: 10.25923/enp8-6w06

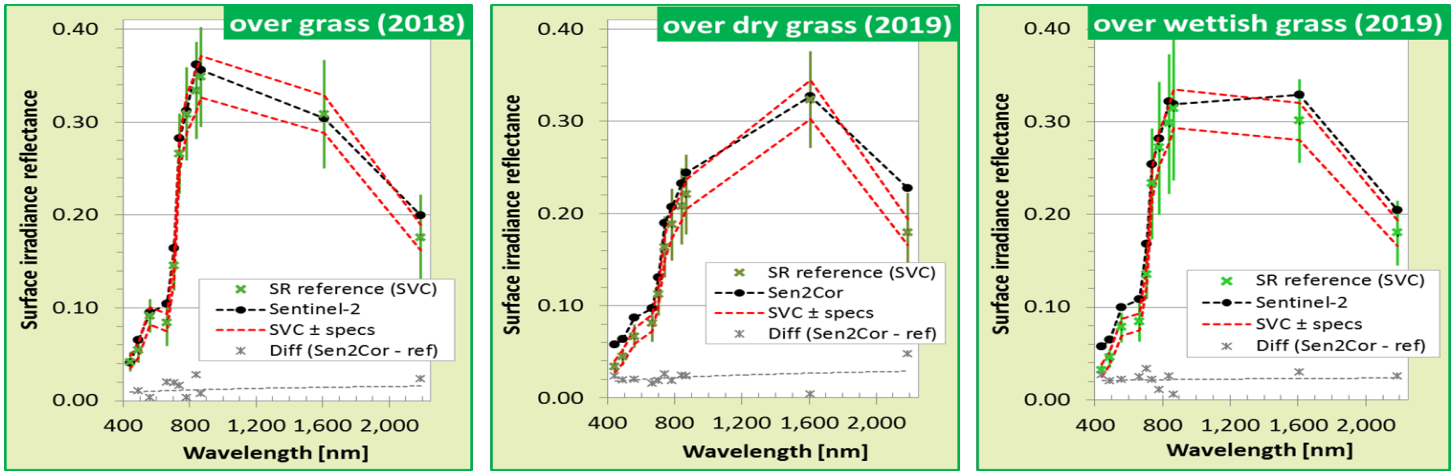

Figure 2: Comparison of SR reference averaged from measurements on ground (green crosses) with SR spectra retrieved from Sentinel-2 data (black dashed line). Green vertical 'Error bars' are standard deviation of measurements on ground representing the natural variability of the SR of the meadow. Red dashed lines frame the range of uncertainty allowed by specification $|\Delta SR| \leq 0.05 * SRref + 0.005$. Grey dashed line gives the difference of SR retrieved from Sentinel-2 and reference.

4. Comparison Results

Copernicus Sentinel-2 data were processed with Sen2Cor 2.8 public version for comparison. Spatial averages of AOT_{550} and WV maps from Sen2Cor over 9 x 9 km^2 ROI around the measurement location give 0.06 and 0.48 cm in 2018, which is in good agreement with the time average from Microtops sunphotometers of 0.07 resp. 0.59 cm. Both AOT_{550} and WV had been higher in 2019 with values 0.17 and 1.28 cm from Sen2Cor. Whereas agreement of WV to reference value 1.38 cm is equivalent to 2018, agreement of AOT_{550} is poorer. The time averaged calculation gives AOT_{550} of 0.23 as reference value. However, a plot of AOT_{550} over time interval shows slow increasing AOT_{550} from morning to noon with two outliers around the time of the overpass time. These two sunphotometer measurements were done a short time after clouds crossed the line of sight to the sun. They are obviously still influenced by the proximity to the clouds. Time interpolation of AOT_{550} to overpass time excluding the two outliers gives AOT_{550} = 0.18 which is again in close agreement to retrieval from Sentinel-2 data (cf. Figure 1).

Figure 2 shows the comparison of SR retrieval from Sentinel-2 data with SR measurements on ground in parallel to Copernicus Sentinel-2 overpasses. All three examples show a small under correction of SR with Sen2Cor, which is larger for data from 2019 than for 2018. RMSD between retrieval and reference is 0.015 for 2018, 0.024 for dry grass in 2019 and 0.023 for wettish grass in 2019. This larger undercorrection in 2019 may be due to the difference between AOT-retrieved for the whole image and the increased AOT at the area of interest during the overpass. The offset between SR retrieval and the reference measurements does not degrade the correctness of shape of SR spectra. The shape is reproduced very well for all three examples shown by high correlation with values 0.996 for 2018, 0.993 for dry grass 2019 and 0.998 for wettish grass 2019. Offset between SR retrieval and reference measurement varies less for examples of 2019 compared to 2018 and varies less for bands in the visible region than in other parts of spectrum. It is worth to mention that bands B05, B11 and B12 don't perform worse than other bands in the given examples. Such behavior was observed in comparison of SR retrieval of Sen2Cor with computed reference data [13].

5. Summary

SR measurements performed on ground in vegetated area in Northern Germany were compared with surface reflectance retrieved from Sentinel-2 data using atmospheric correction processor Sen2Cor. SR is slightly under corrected with RMSD up to 0.025. Shape of SR spectra is reproduced very well with correlation higher than 0.99. This gives rise to the expectation that band indices computed from Sentinel-2 Level-2A Surface Reflectance Product have high accuracy and are very useful for downstream applications.

This study will be continued with more measurements during future years and it will be supplemented by use of SR reference data from different RadCalNet sites [14].

ACKNOWLEDGEMENTS:

The research was performed as part of the Copernicus Sentinel-2 Mission

Return to Page One

Performance Center activities which are managed by ESA.

References

1.Immitzer, M., et al., *Optimal Input Features for Tree Species Classification in Central Europe Based on Multi-Temporal Sentinel-2 Data.* Remote Sensing, 2019. **11**(22): p. 2599 %* http://creativecommons.org/licenses/by/3.0/ %U https://www.mdpi.com/2072-4292/11/22/2599.
2. Askar, et al., *Estimating Aboveground Biomass on Private Forest Using Sentinel-2 Imagery.* Journal of Sensors, 2018.
3.Farahmand, N. and V. Sadeghi, *Estimating Soil Salinity in the Dried Lake Bed of Urmia Lake Using Optical Sentinel-2 Images and Nonlinear Regression Models.* Journal of the Indian Society of Remote Sensing, 2020. **48**(4): p. 675-687.
4. Li, Y., et al., *Evaluation of Sentinel-2A Surface Reflectance Derived Using Sen2Cor in North America.* Ieee Journal of Selected Topics in Applied Earth Observations and Remote Sensing, 2018. **11**(6): p. 1997-2021 %U https://ieeexplore.ieee.org/document/8386426/.
5. Toming, K., et al., *First Experiences in Mapping Lake Water Quality Parameters with Sentinel-2 MSI Imagery.* Remote Sensing, 2016. **8**(8).
6.Dornhofer, K., et al., *Water Constituents and Water Depth Retrieval from Sentinel-2A-A First Evaluation in an Oligotrophic Lake.* Remote Sensing, 2016. **8**(11).
7.Richter, R., Louis, J., Müller-Wilm, U., *Sentinel-2 MSI—Level 2A Products Algorithm Theoretical Basis Document*. 2012, Telespazio VEGA Deutschland, GmbH, Darmstadt, Germany.
8.Louis, J., et al., *Integration and Assimilation of Meteorological (Ecmwf) Aerosol Estimates into Sen2cor Atmospheric Correction.* Igarss 2018 - 2018 Ieee International Geoscience and Remote Sensing Symposium, 2018: p. 1894-1897.
9.Schlapfer, D., et al., *Atmospheric precorrected differential absorption technique to retrieve columnar water vapor.* Remote Sensing of Environment, 1998. **65**(3): p. 353-366.
10. Louis, J., *Sentinel 2 MSI - Level 2A Product Definition*. 2016.
11. Corporation, S.V. April 29, 2020]; Available from: https://www.spectravista.com/our-instruments/hr-1024i/.
12. Morys, M., et al., *Design, calibration, and performance of MICROTOPS II handheld ozone monitor and Sun photometer.* Journal of Geophysical Research-Atmospheres, 2001. **106**(D13): p. 14573-14582.
13. Pflug, B., et al., *Radiometric performance assessment of Sen2Cor version 2.8*, in *3rd Sentinel2 Validation Team-Meeting*. 2019: Toulouse, France.
14.Bouvet, M., et al., *RadCalNet: A Radiometric Calibration Network for Earth Observing Imagers Operating in the Visible to Shortwave Infrared Spectral Range.* Remote Sensing, 2019. **11**(20).

Discuss the Article

Towards harmonization of multi-sensor time series: radiometric Top-of-Atmosphere reflectance consistency assessment

By Sindy Sterckx and Erwin Wolters (Flemish Institute for Technological Research, VITO)

Introduction

High spatial resolution missions, such as Sentinel-2 and Landsat-8, open opportunities to set up operational Earth Observation services at local scale. To overcome cloud coverage issues and relatively low revisit frequencies, data from different missions are often combined, which requires the need for data interoperability. By data interoperability we mean that the sensors are radiometrically inter-calibrated, so that the higher level products are not influenced by differences in sensor characteristics (such as spectral response differences) or processing algorithms. The aim of the Belharmony project (https://belharmony.vito.be) is to assess and improve the consistency of multi-sensor high resolution time series generated on the basis of the following sensors: Deimos-1, Sentinel-2 (S2), Landsat-8 (LS8) and PROBA-V (PV), in which for PROBA-V only data from the CENTER camera, which provides

Return to Page One

doi: 10.25923/enp8-6w06

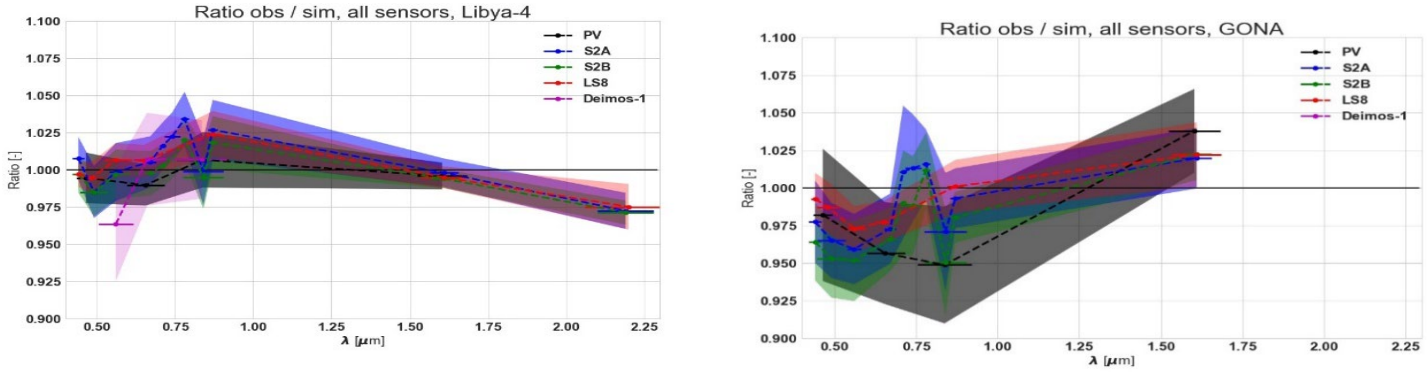

Figure 1: Mean ratio (over all observations) of the satellite-measured top-of-atmosphere (TOA) reflectances to the 6SV TOA reflectance simulations over Libya-4 (left) and over Gobabeb (GONA) RadCalNet site (right). The shaded areas denote the 1 standard deviation of the obtained ratios. The horizontal bars indicate the spectral band widths of the respective sensors. The mean ratio was calculated over the following number of Libya-4 (GONA) observations: 68 (27) S2A, 19 (22) S2B, 62 (14) LS8, 214 (42) PV and 91 (0) Deimos-1.

100 m spatial resolution with a 5 day revisit time, are considered. The harmonization of the multi-sensor time series within Belharmony consists of

1. the assessment and correction of radiometric biases at TOA (Top-of-Atmosphere) through application of a set of independent vicarious calibration methods,
2. the derivation of spectral response adjustment factors, to compensate for differences in the relative spectral response functions, and
3. the use of a common processing chain.

This paper focuses on the first aspect, i.e., the assessment of differences in the TOA observations provided by the above introduced satellite instruments (i.e., PV, S2A/S2B, LS8, and Deimos-1). It summarizes the methodology and results described in detail in Sterckx and Wolters (2019).

Assessment of the radiometric consistency over Libya-4 and RadCalNet sites

To assess the TOA reflectance consistency, two approaches were evaluated : 1) the application of the optical sensor calibration with simulated radiances (OSCAR) Libya-4 desert approach and 2) the use of the RadCalNet portal data.

In the OSCAR Libya-4 approach (Govaerts et al., 2013), simulated TOA bidirectional reflectance factors (BRFs) define an absolute reference against which optical sensors can be cross-calibrated. The simulated TOA BRFs are calculated with 6SV, with as input Rahman–Pinty–Verstraete (RPV) Bi-Directional Reflectance Distribution Factor (BRDF) model parameters derived for the Libya-4 desert site, meteorological input data and aerosol characterisation data derived from Aerosol Robotic Network (AERONET) stations in the Sahara region. The modeled TOA reflectance values are simulated for the actual illumination and observation geometry and by taking into account the actual spectral response curves of the sensors. The OSCAR Libya-4 calibration method is applied to S2A, S2B, LS8, Deimos-1, and PROBA-V cloud-free TOA extractions over the Libya-4 region of interest.

RadCalNet comprises a set of four Land Equipped Sites (LES): Railroad Playa (USA, RVUS), Baotou (China), La Crau (France, LCFR), and Gobabeb (Namibia, GONA). The Baotou site was not included in this study, due to the small size of the representative area. For each sensor, cloud-free TOA reflectances were extracted over the RadCalNet sites. For Deimos-1 the provided DNs were first converted to TOA radiances using the gain and bias given in the accompanying file and then the TOA radiances were converted to TOA reflectances using the Thuillier irradiance data (Thuillier et al., 2003). For PROBA-V and S2 the TOA reflectance is directly extracted from the L1C products, while for LS8 the TOA reflectance was calculated from the digital counts using first the rescaling coefficients in the corresponding MTL file and then a correction for the solar zenith angle was applied. Subsequently, the sensor-measured TOA reflectances were compared to the corresponding simulated nadir TOA reflectances extracted from the RadCalNet portal. To allow for direct inter-comparison to the measured TOA reflectances, the RadCalNet-simulated TOA reflectances provided at 10 nm spectral resolution were first interpolated to 1 nm

Return to Page One

doi: 10.25923/enp8-6w06

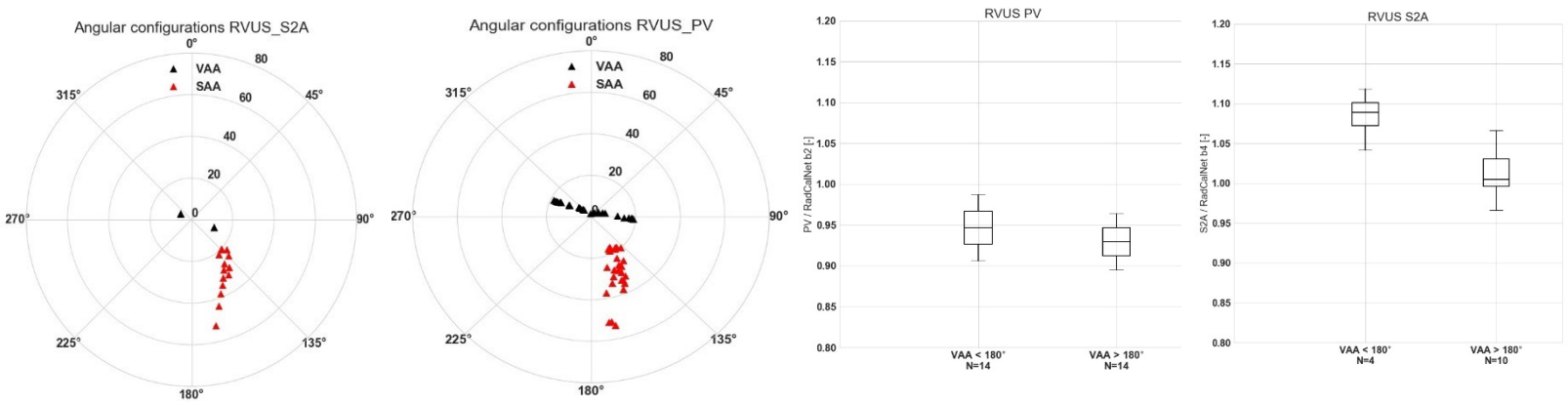

Figure 2: (Left) Observation and illumination geometries for PROBA-V and S2A over RVUS. (Right) Box-whisker plots for the RED channel of the observed/Radcalnet-simulated TOA reflectance ratios over RVUS. Results are divided into classes with VAA < 180° and VAA > 180°. The horizontal line represents the median value, whereas the lower and upper box boundaries denote the 25th and 75th percentiles, respectively. Lower and upper whiskers represent the 5th and 95th percentiles, respectively.

resolution and then convoluted to the S2A, S2B, LS8, Deimos-1, and PROBA-V spectral bands, taking into account their actual spectral response curves.

Figure 1 shows the mean ratios (over all observations) of the satellite-measured TOA reflectances to the simulated TOA reflectances over Libya-4 and over the Gobabeb (GONA) RadCalNet site. For similar RadCalNet sites we refer to Sterckx and Wolters (2019). In view of the data consistency objective and to exclude intrinsic biases in the TOA reflectance reference simulations, we discuss the results relatively to S2A. According to the Libya-4 OSCAR results, LS8, PV, S2B, and Deimos-1 agree with S2A to within ±2% for comparable spectral bands, with the exception of the Deimos-1 Green band, which is approximately 3.5% lower than S2A. Deviations observed between S2A and S2B are of the same magnitude as those observed between S2A and the other missions. For most bands, S2A is slightly brighter than S2B which is in line with results reported by Revel et al (2019) and Helder et al. (2018).

Significantly larger scatter is observed in the RadCalNet results (see also Sterckx and Wolters, 2019), both within (*intra-sensor*) and between sensors (*inter-sensor*). Further investigation showed that BRDF effects strongly influence the RadCalNet results. Polar plots of the viewing and illumination geometries for S2A, S2B, PROBA-V, and Deimos-1 made for the various RadCalNet sites showed that only Landsat-8 observes the various sites under almost nadir viewing conditions (i.e., VZA < 1°). For S2A and S2B, the VZA is generally <10°, but over LCFR and RVUS the S2A and S2B viewing azimuth angle (VAA) is alternating between ~135° and ~270° (see Figure 2). For Deimos-1, the VAA also alternates between ~80° and ~280°, while for PROBA-V the VAA range changes more continuously between ~100° and ~280°. To further analyze the impact of the changing viewing azimuth angle, we divided the ratios of observed/RadCalNet-simulated TOA reflectances into two groups: VAA < 180° and VAA > 180°. These subsets are presented in Figure 2 as box-whisker plots for the RED spectral range of PROBA-V and S2A over RVUS. A clear difference in the TOA reflectance depending on the VAA can be seen. This *intra-sensor* difference is significantly larger than the *inter-sensor* differences observed for instance between S2A and S2B.

Conclusion and recommendations

Libya-4 OSCAR desert calibration results for LS8, PROBA-V, Deimos-1, S2A, and S2B agree to within ±2% for comparable spectral bands, with the exception of the Deimos-1 Green band. S2A is slightly brighter than S2B for most bands. Results confirm that all sensors investigated are well calibrated and that *inter-sensor* differences are minor, at least over the bright Libya-4 site. No consistent results could be obtained over the RadCalNet sites for the sensors investigated. BRDF effects significantly influence the observed results, as many of the satellite observations are made under non-nadir conditions. Even for slightly off-nadir VZAs of ~7°, a difference in the TOA measured reflectance values over RVUS and LCFR could be observed between Eastern and Western viewing directions. In order to fully explore the potential of the RadCalNet sites, it is recommended that BRDF characterizations be additionally incorporated into the RadCalNet simulations and made publicly available through the distribution portal.

Return to Page One

References

Govaerts, Y.; Sterckx, S.; Adriaensen, S. Use of simulated reflectances over bright desert target as an absolute calibration reference. Remote Sens. Lett. 2013, 4, 523–531.

Helder, D.; Markham, B.; Morfitt, R.; Storey, J.; Barsi, J.; Gascon, F.; Clerc, S.; LaFrance, B.; Masek, J.; Roy, D.P.; et al. Observations and Recommendations for the Calibration of Landsat 8 OLI and Sentinel 2 MSI for Improved Data Interoperability. Remote Sens. 2018, 10, 1340.

Revel, C.; Lonjou, V.; Marcq, S.; Desjardins, C.; Fougnie, B.; Coppolani-Delle, C.; Guilleminot, N.; Lacamp, A.; Lourme, E.; Miquel, C.; et al. Sentinel-2A and 2B absolute calibration monitoring, Eur. J. Remote Sens. 2019, 52, 122–137, doi:10.1080/22797254.2018.1562311.

Sterckx, S.; Wolters, E. Radiometric Top-of-Atmosphere Reflectance Consistency Assessment for Landsat 8/OLI, Sentinel-2/MSI, PROBA-V, and DEIMOS-1 over Libya-4 and RadCalNet Calibration Sites. Remote Sens. 2019, 11, 2253, **https://doi.org/10.3390/rs11192253**.

Thuillier, G., Hersé, M., Labs, D. et al. The Solar Spectral Irradiance from 200 to 2400 nm as Measured by the SOLSPEC Spectrometer from the Atlas and Eureca Missions. Solar Physics 214, 1–22 (2003). https://doi.org/10.1023/A:1024048429145

Discuss the Article

NEWS IN THIS QUARTER

The new Copernicus digital elevation model

By Peter Strobl (European Commission/JRC)

Most observations of the Earth's surface are directly or indirectly influenced by its three-dimensional geometry and therefore a Digital Elevation Model (DEM) is a prerequisite for the proper calibration and analysis of most Earth Observation (EO) data sets.

For a large EO program like Copernicus, quality, availability and consistency of the used DEM data are a horizontal topic affecting most areas of data production and analysis. Already in 2009, then still called GMES, Copernicus undertook to procure the first complete, consistent and publicly available European DEM at 1" (~30m) resolution. The EU-DEM rapidly became one of the most downloaded items of the Copernicus Land Monitoring Service portal. Used for a broad range of applications, it clearly clearly testified the necessity of a respective reference data set within the program and beyond. With the launch of Sentinel-2A in June 2015, Copernicus opened a new era of unprecedented volume and quality of fine scale (10m) EO data.

Table 1: The three main instances of the Copernicus DEM

Instance Code	Spatial Extent	Sampling	License Type
GLO-90-F	Global	90 m	Full, Free & Open
GLO-30-R	Global	30 m	Restricted
EEA-10-R	EEA39	10 m	Restricted

The orthorectification of the acquired imagery however requires a DEM of global extent, high resolution and fidelity [1]. The status quo DEM used for this purpose at ESA so far has been a proprietary product selected based on a study from 2011 and was primarily based on SRTM data. Various new initiatives providing global DEM data have been announced since then, some of which foresee adopting a 'free & open' policy at least to certain qualities or extents of the data. Some parts of the Copernicus program started utilizing different such data sets.

Recently, with the establishment of the final Sentinel-2 (S2) geometry and the subsequent need of a state-of-the-art global DEM satisfying the key requirements of S2 orthorectification, a unique window to address the issue has opened. Consequently, the European Commission as program owner of copernicus, decided to acquire a new, globally consistent DEM, suitable as a reference across the whole programme and guaranteeing the Copernicus user The European Space Agency was put in charge of the procurement of the official Copernicus DEM, which now WorldDEM(TM) is a standardised global and high-precision Digital Surface

Return to Page One

doi: 10.25923/enp8-6w06

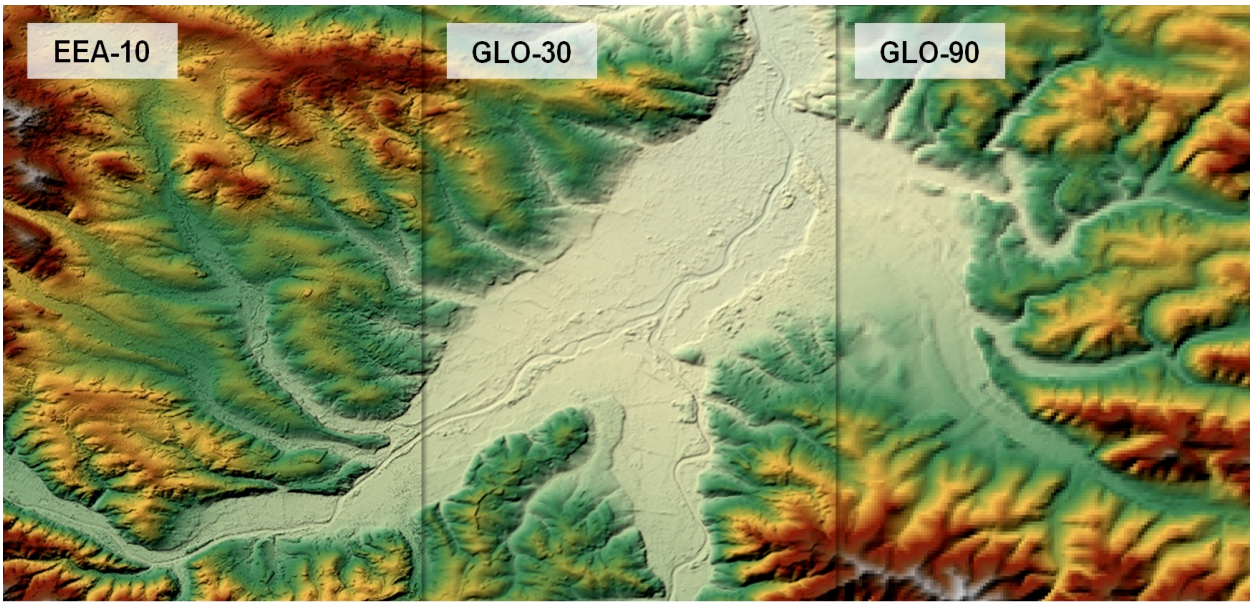

Figure 1: Visual comparison of Copernicus DEM instances (left: EEA-10 | centre: GLO-30 | right: GLO-90) © DLR e.V. 2016 and © Airbus Defence and Space GmbH 2019 provided under COPERNICUS by the European Union and ESA; all rights reserved.

Model (DSM) derived from the TanDEM-X mission data in close cooperation with the German Aerospace Center (DLR) which undertook a thorough accuracy assessment[2].

The Copernicus DEM includes a portfolio of individual data layers addressed at different user groups and applications and supplemented by comprehensive metadata describing data provenance and quality down to the pixel level and following as much as possible DGED and INSPIRE standards. Its backbone consists of three instances with different sampling distance, use policy and extent [See Table1].

The 90 meter dataset comes with a free license following the Copernicus free, full and open data policy. The 30 meter and 10 meter dataset are restricted to eligible entities and usage within the programme. Detailed technical documentation (Product Handbook, Validation Report) and access guidelines are available through the Copernicus Space Component Data Access site.

The arrival of the Copernicus DEM has also triggered an effort by the Committee on Earth Observing Satellites (CEOS) to compare globally available DEMs and give recommendations on their use in various applications. Further information can be found on the home page of Terrain Mapping SubGroup to the CEOS Working Group on Calibration and Validation.

References

[1] Ressl, C., Pfeifer, N., 2018. "Evaluation of the elevation model influence on the orthorectification of Sentinel-2 satellite images over Austria." European Journal of Remote Sensing, 51, 693-709.

[2] Rizzoli, P., Martone, M., Gonzalez, C., Wecklich, C., Borla Tridon, D., Bräutigam, B., et al. (2017). "Generation and performance Assessment of the global TanDEM-X Digital Elevation Model. ISPRS." Journal of Photogrammetry and Remote Sensing, 132, 119–139.

Discuss the Article

Return to Page One

doi: 10.25923/enp8-6w06

Announcements

EUMETSAT Meteorological Satellite Conference 2020 Cancelled

By Tim Hewison (EUMETSAT)

In view of the current COVID-19 situation and the expected travel restrictions for the whole year, after consultation of DWD, EUMETSAT has come to the conclusion that an in-person meeting will unfortunately not be possible in autumn 2020. We have therefore decided to cancel the 2020 EUMETSAT Meteorological Satellite Conference that was foreseen to take place in Würzburg, Germany from 28 September to 2 October. We thank all of you for the interest, the investment of time you have already taken in writing or reviewing abstracts and apologise for any inconvenience this may cause. We will be very pleased to welcome you to next year's conference in Bucharest from 20-24 September 2021

GSICS-Related Publications

Buehler, S. A., Prange, M., Mrziglod, J., John, V. O., Burgdorf, M., & Lemke, O. (2020). Opportunistic constant target matching—A new method for satellite intercalibration. Earth and Space Science. 7, e2019EA000856. https://doi.org/10. 1029/2019EA000856

C. Wu *et al*., "FY-3D HIRAS Radiometric Calibration and Accuracy Assessment," in *IEEE Transactions on Geoscience and Remote Sensing*, vol. 58, no. 6, pp. 3965-3976, June 2020, doi: 10.1109/TGRS.2019.2959830

Hewison, T.J.; Doelling, D.R.; Lukashin, C.; Tobin, D.; O. John, V.; Joro, S.; Bojkov, B. Extending the Global Space-Based Inter-Calibration System (GSICS) to Tie Satellite Radiances to an Absolute Scale. *Remote Sens.* **2020**, *12*, 1782.

Ma, J.; Guo, J.; Ahmad, S.; Li, Z.; Hong, J. Constructing a New Inter-Calibration Method for DMSP-OLS and NPP-VIIRS Nighttime Light. *Remote Sens.* **2020**, *12*, 937.

Merchant, C.J., T. Block, G.K. Corlett, O. Embury, J.P.D. Mittaz, and J.D.P. Mollard.'Harmonization of Space-Borne Infra-Red Sensors Measuring Sea Surface Temperature'. *Remote Sensing* 12, no. 6 (2020). https://doi.org/10.3390/rs12061048.

Rosenkranz, Philip W., William J. Blackwell, and R. Vincent Leslie. 'Climate-Quality Calibration for Low Earth-Orbit Microwave Radiometry'. *Remote Sensing* 12, no. 2 (2 January 2020): 241. https://doi.org/10.3390/rs12020241.

Tonooka, H.; Sakai, M.; Kumeta, A.; Nakau, K. In-Flight Radiometric Calibration of Compact Infrared Camera (CIRC) Instruments Onboard ALOS-2 Satellite and International Space Station. *Remote Sens.* **2020**, *12*, 58.

Zeng, Z.-Q., and G.-M. Jiang. 'Intercalibration of FY-3C MWRI against GMI Using the Ocean Microwave Radiative Transfer Model'. *IEEE Access* 8 (2020): 63320–35. https://doi.org/10.1109/ACCESS.2020.2984090.

Submitting Articles to the GSICS Quarterly Newsletter:

The GSICS Quarterly Press Crew is looking for short articles (800 to 900 words with one or two key, simple illustrations), especially related to calibration / validation capabilities and how they have been used to positively impact weather and climate products. Unsolicited articles may be submitted for consideration anytime, and if accepted, will be published in the next available newsletter issue after approval / editing. Please send articles to manik.bali@noaa.gov.

Return to Page One

doi: 10.25923/enp8-6w06

With Help from our friends:

The GSICS Quarterly Editor would like to thank the Editors of this Special Issue: Zolti Szantoi (EC/JRC), Valentina Boccia (ESA) and Carine Quang (CS Group).
A special thanks for our expert reviewers Dave R. Doelling (NASA), Larry Flynn (NOAA), Tim Hewison (EUMETSAT), Likun Wang (NOAA) and Manik Bali (NOAA) for reviewing articles in this issue.

Published By

GSICS Coordination Center
NOAA/NESDIS/STAR NOAA
Center for Weather and Climate Prediction, C
5830 University Research Court, C2850
College Park, MD 20740, USA

Return to Page One